ACS central science

http://pubs.acs.org/journal/acscii

Research Article

Near-Zero-Energy Smart Battery Thermal Management Enabled by Sorption Energy Harvesting from Air

Jiaxing Xu,[†] Jingwei Chao,[†] Tingxian Li,*[,†] Taisen Yan, Si Wu, Minqiang Wu, Bingchen Zhao, and Ruzhu Wang*

Cite This: *ACS Cent. Sci.* 2020, 6, 1542−1554

Read Online

ACCESS | Metrics & More | Article Recommendations | Supporting Information

ABSTRACT: Effective battery thermal management (BTM) is critical to ensure fast charging/discharging, safe, and efficient operation of batteries by regulating their working temperatures within an optimal range. However, the existing BTM methods not only are limited by a large space, weight, and energy consumption but also hardly overcome the contradiction of battery cooling at high temperatures and battery heating at low temperatures. Here we propose a near-zero-energy smart battery thermal management (SBTM) strategy for both passive heating and cooling based on sorption energy harvesting from air. The sorption-induced reversible thermal effects due to metal−organic framework water vapor desorption/sorption automatically enable battery cooling and heating depending on the local battery temperature. We demonstrate that a self-adaptive SBTM device with MIL-101(Cr)@carbon foam can control the battery temperature below 45 °C, even at high charge/discharge rates in hot environments, and realize self-preheating to ∼15 °C in cold environments, with an increase in the battery capacity of 9.2%. Our approach offers a promising route to achieving compact, liquid-free, high-energy/power-density, low-energy consumption, and self-adaptive smart thermal management for thermo-related devices.

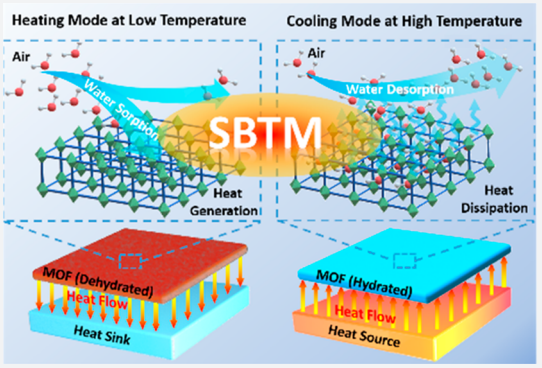

INTRODUCTION

High-energy-density rechargeable batteries, especially lithium-ion batteries (LIBs), have attracted wide interest with the emergence of electric vehicles (EVs) and consumer electronics due to their desirable energy densities, long lifetimes, and low self-discharge rates.[1−3] To maintain safe and high-performance operation, LIBs need to work under a moderate temperature ranging from −20 to 60 °C, ideally within a more restrictive temperature range between 20 and 40 °C.[4,5] The high energy densities of LIBs incur potentially strong exothermic effects that lead to an apparent temperature increase. Moreover, high-rate charging is the general trend for shortening the charging duration of batteries, but it causes an inevitable temperatures increase in LIBs.[6,7] The elevated temperature accelerates the degeneration of the cathode and the growth of the solid-electrolyte interphase (SEI) in LIBs and thus results in capacity fading and internal resistance increment.[8] Remarkably, LIBs face the safety risks of overheating and thermal runaway if they work under high temperatures for a long duration.[9,10] However, a low ambient temperature also threatens the working performance and safe operation of LIBs because the diffusion kinetics of Li^+ ions becomes slow and Li metal deposition occurs.[11] As a result, LIBs suffer from significant performance degradation in terms of both energy power and energy density, thus causing issues for EV applications in cold regions, especially during the start-up stage of EVs. Therefore, battery cooling at high temperatures and battery heating at low temperatures are simultaneously required to achieve highly efficient and safe operation of LIBs under various climate conditions.

To address the above challenges, various battery thermal management (BTM) systems have been developed in the past decades to regulate LIB temperatures within an optimal range.[12] For the active BTM strategies, traditional air-forced cooling suffers from a low cooling power when used for heat dissipation of high-energy-density LIBs, especially under extreme operating conditions. Liquid cooling is another commercial approach with a stronger heat dissipation ability, but its high performance is realized at the expense of a large weight, a complex structure, and extra electricity consumption.[13] Moreover, the extra onboard battery bank electricity consumption shortens the driving range of EVs. In recent years, passive BTM strategies based on solid−liquid phase-

Received: May 6, 2020
Published: August 14, 2020

https://dx.doi.org/10.1021/acscentsci.0c00570
ACS Cent. Sci. 2020, 6, 1542−1554

change materials (PCMs) have been regarded as another efficient approach to regulate the battery temperature by utilizing the large endothermic enthalpies of these materials during the phase transformation from solid to liquid states (220−251 kJ kg^{-1} for paraffin wax melting).[14] The PCM-based passive strategies have many advantages, such as fast temperature control, excellent temperature uniformity, and low energy consumption. To overcome the major disadvantage of poor thermal transfer performance, recent studies have been devoted to enhancing the thermal conductivity of PCMs by synthesizing phase-change composites with highly conductive additives.[15−17]

Compared with solid−liquid phase-change processes, liquid−gas phase-change processes show much higher heat dissipation capacities due to the high latent heats (∼2400 kJ kg^{-1} for water evaporation).[18] Heat pipe cooling systems based on boiling−condensation (liquid−gas phase change) have been widely applied in many consumer electronics, but the high cost and small contact area for heat exchange restrict the large-scale application of these systems in BTM for EVs.[19] In recent years, evaporating-based BTM systems were proposed for specific hybrid electric vehicles (HEVs), where batteries were submerged in liquid fuels (e.g., propane or ammonia) to prevent overheating and thermal runaway. The liquid fuels are heated to vaporization by absorbing the heat from batteries with increasing temperature; thereafter, the warm vapor is used to fuel the engine to achieve a higher combustion efficiency.[20] Recently, another novel water evaporation-based BTM system was reported to control the temperature of LIBs by using superabsorbent polymers to store liquid water and was fixed on the external surface of LIBs.[21,22] With increasing temperature, water vapor is released from the polymers and then diffuses to the ambient air, removing a large amount of heat from the batteries to the surroundings. Such water evaporation-based BTM systems have the distinct advantages of high cooling power and low energy consumption; however, they have the risk of short-circuiting and need an extra water storage tank to supply the liquid water to ensure the continuous water evaporation process for battery cooling during operation. In addition, water desorption of sorbents to realize the temperature control of electronic devices with high cooling power was recently reported,[23] but its cooling duration is strongly dependent on the amount of employed sorbent, and thus it has the similar risk of losing effectiveness for continuously cooling electronic devices at high temperatures. Benefiting from the automatic water recovery by sorption from moisture, similar desorption cooling strategies for the smart temperature regulation of the soft machine[24] and the cooling of the photovoltaic (PV) panel[25] have been proposed recently; however, research on sorption-based BTM has not yet been reported.

Most studies in the past decade have focused on battery cooling, and less attention has been paid to battery heating to improve the energy power and energy density of LIBs in cold regions. The major commercial heating strategies are external air heating or liquid heating with electricity consumption, and they show high energy consumption and low heating efficiencies.[26] Moreover, the onboard battery bank electricity consumption of the heating systems would shorten the driving range of EVs by as much as 22%.[27] Thus controlling the battery temperature under various climate conditions using one BTM method is a severe challenge. Recently, a shape memory alloy (SMA)-actuated interfacial thermal regulator was reported for passive BTM in both hot and cold extreme environments.[28] The SMA-actuated thermal regulator can enable LIB cooling or heating by maintaining the thermal conduction or insulation between the LIBs and the air-cooled heat sink with SMA wires. This passive BTM method has the superiority of simple operation and can enhance the capacity of LIBs in cold weather by retaining the battery self-generated heat through thermal insulation. However, the cooling power for thermal dissipation is still limited by the air-cooled heat sink, and thus auxiliary refrigeration devices are needed if it is used for high-power battery cooling. Furthermore, the preheating of the battery during the start-up stage is of vital importance for EV applications in cold regions, delivering much higher discharging power;[29] therefore, both the preheating of the battery in the start-up stage and its thermal regulation in the operation stage are necessary to ensure high energy densities and long lifetimes of the battery at low ambient temperatures.

Herein we report a novel near-zero-energy smart battery thermal management (SBTM) strategy to regulate the battery temperature in both hot and cold environments. Battery heating or cooling is automatically switched in response to the local battery temperature based on the water sorption or desorption states of the sorbent. The sorption-induced reversible thermal effects enable passive battery cooling or heating for SBTM without any additional energy input. The liquid-free operation makes the sorption-based SBTM strategy very suitable for the thermal management of electronic devices/batteries. Moreover, the SBTM strategy exhibits the distinct advantages of high-energy/power-density, self-adaptive, and real-time adjustment of cooling/heating for BTM. We first introduce the mechanism of sorption-based smart thermal management, screen out the most suitable sorbent for SBTM, and then show the feasibility of near-zero-energy smart thermal management by employing MIL-101(Cr) in a proof-of-concept device under simulated conditions. Finally, we demonstrate sorption-based SBTM applications for the thermal management of commercial 18650 LIBs at different ambient temperatures from 10 to 40 °C and different charge/discharge rates from 1 to 3 C.

RESULTS AND DISCUSSION

Operating Mechanism of Sorption-Based Smart Thermal Management. Solid−gas sorption has been widely investigated and applied in water sorption-based refrigeration,[30] thermal energy storage,[31] heat pumps,[32] and thermal batteries[33] due to the reversible exothermic/endothermic heat effects during the gas sorption/desorption processes. However, BTM applications based on reversible sorption energy harvesting from air are lacking. In recent years, water vapor sorption from air has attracted much attention for atmospheric water harvesting[34−36] and energy harvesting[37,38] due to the intrinsic large water vapor storage in ambient air. The enthalpy difference between the vapor-state water in air and the sorption-state water in a sorbent brings about a large amount of potential energy resources that are rarely exploited.

We propose a sorption-based smart thermal management strategy based on reversible sorption energy harvesting from air, as conceptually shown in Figure 1a. A suitable sorbent is coated on the surface of electronic devices/batteries, and it can undergo sorption or desorption processes in response to low or high temperature. For the cooling mode at high temperatures, the heat released by electronic devices/batteries is first

https://dx.doi.org/10.1021/acscentsci.0c00570
ACS Cent. Sci. 2020, 6, 1542−1554

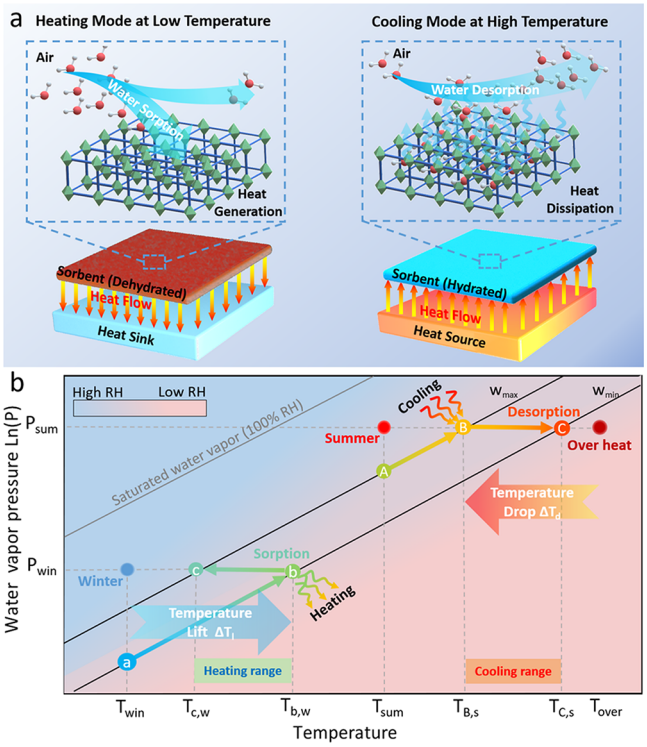

Figure 1. Smart thermal management based on reversible sorption energy harvesting from air. (a) Schematic of smart thermal management using porous sorbents. The sorbent coated on the electronic device/battery automatically performs the water sorption or desorption process depending on the operating temperature of the device and ambient conditions. The thermal dissipation by water desorption to air provides desorption cooling effects at high temperatures (right side), while the thermal harvesting by water sorption from air provides sorption heating at low temperatures (left side). (b) Pressure−temperature diagram showing the self-regenerative reversible sorption energy-harvesting cycles at heating and cooling modes. For the cooling mode (A−B−C) in the hot environment (e.g., summer), the sorbent removes the heat released by the electronic device/battery under the operation stage in the form of desorption heat to drive water desorption to air. Point A is the saturated state of the sorbent at T_{sum}. Point B is the initial state of water desorption with the lowest temperature ($T_{B,s}$) for cooling. Point C is the end state of water desorption with the highest temperature ($T_{C,s}$) for cooling. For the heating mode (a−b−c) in the cold environment (e.g., winter), the sorbent adsorbs water from the air and generates sorption heat used to preheat the electronic device/battery from a low temperature, T_{win}, to a suitable working temperature with a heating range between $T_{c,w}$ and $T_{b,w}$. Point a is the dry state of the sorbent at T_{win} (isolated from moisture). Point b is the initial state of water sorption with the highest temperature ($T_{b,s}$) for heating. Point c is the end state of water sorption with the lowest temperature ($T_{c,s}$) for heating.

transferred to the hydrated sorbent and then dissipated to break the sorbent−water bonds (e.g., van der Waals forces, hydrogen bonds, or coordinate bonds), thus leading to water desorption. Heat dissipation (desorption heat of the sorbent) is used to cool the electronic devices/batteries in hot environments, where the hydrated sorbent desorbs water vapor, directly removing heat to ambient air. Conversely, for the heating mode at low temperatures, the dehydrated sorbent adsorbs water vapor from ambient air, generating a large amount of sorption heat through the sorbent−water bond formation during the water sorption process. The generated heat (sorption heat of sorbent) is quickly transferred to heat the electronic devices/batteries in cold environments. In summary, sorption-induced reversible thermal effects enable passive heating or cooling for electronic devices/batteries in cold or hot environments through the switch of the dehydrated and hydrated states of the sorbent.

Figure 1b illustrates a schematic diagram of the self-regenerative reversible sorption energy-harvesting cycles in the heating and cooling modes for sorption-based smart thermal management. The pressure−temperature ($P-T$) equilibrium lines of the sorbent−water sorption pair and isohumes of ambient air can be described by the Clausius−Clapeyron equation

$$\mathrm{Ln}\, P_{water} = A - \frac{\Delta H_{ad}}{RT} \quad (1)$$

where A is a constant value determined by the hydrophilicity of the sorbent, ΔH_{ad} is the water adsorption enthalpy, and R is the gas constant. Two water sorption equilibrium lines representing the sorbents with minimum (W_{min}) and maximum (W_{max}) water contents are plotted. For the cooling mode (A−B−C) in a hot environment (e.g., summer), the heat released by the electronic devices/batteries is absorbed by the sorbent in the form of desorption heat to drive water desorption to ambient air. The electronic devices/batteries will be cooled from a high temperature T_{over} to a low working temperature with a temperature drop of ΔT_d. The water desorption to the ambient air process can be approximately regarded as a water vapor isobaric process ($P = P_{sum}$). The final desorption equilibrium state of the dehydrated sorbent ranges from the left point B with maximum water content of W_{max} to the right point C with minimum water content of W_{min} (B−C). As a result, the cooling range varies between $T_{B,s}$ and $T_{C,s}$. Afterward, the dehydrated sorbent is self-regenerated to the hydrated state by adsorbing water from atmospheric moisture once its temperature becomes low enough for water sorption (the left zone of the W_{max} sorption equilibrium line) during the idle time of the electronic devices/batteries. Thus the hydrated sorbent recovers its water desorption capacity and can reabsorb heat for desorption cooling during the next stage.

For the heating mode (a−b−c) in a cold environment (e.g., winter), the sorption heat released by the sorbent during its water sorption from ambient air is first used to preheat the electronic devices/batteries in the start-up stage. The electronic devices/batteries are heated from a low start-up temperature T_{win} to a high working temperature with a temperature increase of ΔT_l. In contrast with the cooling mode in summer, the final sorption equilibrium state of the hydrated sorbent moves from the right point b with W_{min} to the left point c with W_{max} (b−c) also following a water vapor isobaric process ($P = P_{win}$), and the heating range varies between $T_{c,w}$ and $T_{b,w}$. During the operation phase after the start-up stage, the internal Joule heat produced by the electronic devices/batteries will self-heat them and further increase their working temperatures. Once the working temperature becomes high enough for water desorption (the right zone of the W_{min} sorption equilibrium line), the hydrated sorbent will be regenerated by desorbing water vapor to ambient air. This water desorption can also prevent the safety risk of overheating the electronic devices/batteries during the operation phase. Accordingly, the dehydrated sorbent will again possess a water sorption capacity and can be reutilized for sorption heating during the next stage.

https://dx.doi.org/10.1021/acscentsci.0c00570
ACS Cent. Sci. 2020, 6, 1542−1554

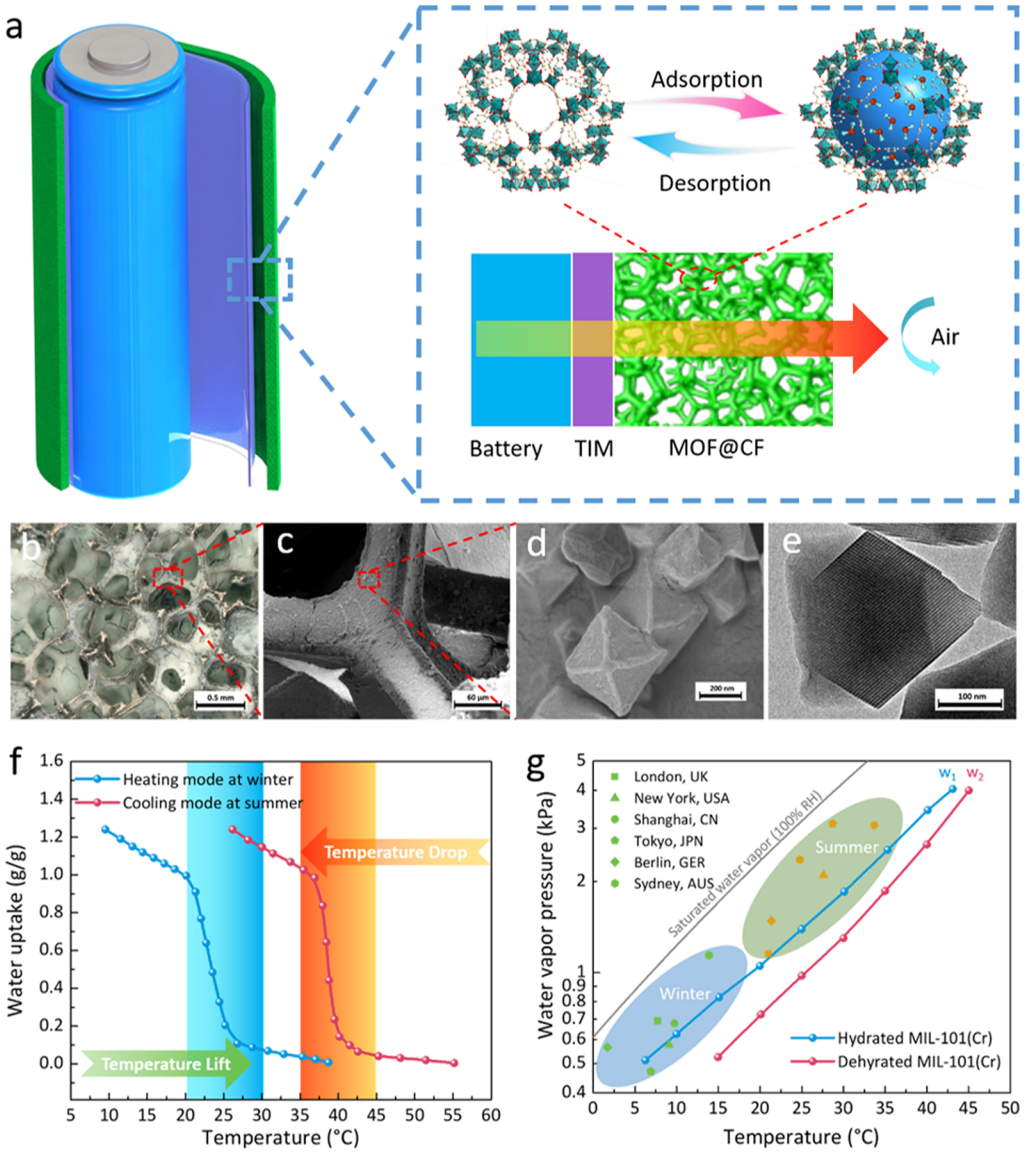

Figure 2. Design of sorption-based SBTM and characterization of MIL-101(Cr) for efficient thermal management to LIBs. (a) Design of MOF sorption-based SBTM for a single LIB. The MIL-101(Cr) is coated on carbon foam (CF) as MOF@CF to enhance the heat and mass transfer performance of MIL-101(Cr). The MOF@CF layer is stuck on the external surface of LIBs by thermal interface material (TIM). (b) Optical microscopic image displaying the uniform coating of MIL-101(Cr) (green part) on CF (dark metal frameworks). (c) SEM image showing MIL-101(Cr) particles adhered on the frameworks of CF. (d) SEM image of MIL-101(Cr) showing the regular octahedral structures of MIL-101(Cr) crystals. (e) TEM image of MIL-101(Cr) crystal presenting its ordered nanoscale pores for water vapor sorption. (f) Water sorption isotherms of MIL-101(Cr) under typical winter conditions (water vapor pressure of 80% RH at 10 °C) and typical summer conditions (water vapor pressure of 60% RH at 30 °C). The large water uptake changes of MIL-101(Cr) within a small temperature swing enable its promising potential for sorption-based BTM. (g) Climate data of typical cities worldwide in winter and summer,[46] together with two water vapor sorption equilibrium lines of MIL-101(Cr) with water contents of 1.0 (blue line) and 0.1 g/g (read line), revealing that MIL-101(Cr) has a wide adaptability for sorption-based SBTM due to its capability of adsorbing water from ambient air to become a saturated adsorption state under winter and summer conditions.

The proposed sorption-based smart thermal management strategy can not only overcome the contradiction of battery cooling requirements at high temperatures and battery heating requirements at low temperatures but also automatically switch between the desorption cooling and sorption heating modes according to the local working temperature and ambient conditions. Moreover, the sorbent can realize self-regeneration between the dehydrated and hydrated states without any additional energy input. Because the solid−gas sorption enthalpy is usually much higher than the solid−liquid or liquid−gas phase-change enthalpies, our proposed sorption-based smart thermal management strategy exhibits the distinct advantages of a high-energy/power-density and near-zero-energy consumption compared with traditional thermal management methods. Furthermore, the liquid-free operation makes it more suitable for the thermal management of batteries.

Sorbent Screening and Characterization for Smart Battery Thermal Management. The sorption equilibrium characteristics of sorbents determine the controllable cooling or heating temperature range (ΔT) for BTM. Furthermore, sorbents must automatically adsorb water from air and desorb water to air at a moderate temperature to realize reversible thermal management. Therefore, the sorbent candidates must

https://dx.doi.org/10.1021/acscentsci.0c00570
ACS Cent. Sci. 2020, 6, 1542−1554

meet several strict restrictions to realize successful thermal management applications: (i) moderate hydrophilicity to adsorb water from air under ambient conditions while desorbing water to air at a suitable working temperature range of thermal management; (ii) an "S" shape (type V) of the water sorption isotherms, allowing reversible sorption−desorption transitions within small temperature swings;[39] (iii) a high water sorption capacity to provide a large amount of heat dissipation or generation; (iv) fast water sorption/desorption kinetics to achieve high heating/cooling powers; and (v) high thermal stability during repeated water sorption−desorption processes.

Traditional microporous sorbents, such as zeolites, show a high desorption temperature (>100 °C) that exceeds the range of thermal management.[40] Although traditional mesoporous sorbents, such as silica gel, have low desorption temperatures, their nearly linear desorption isobars induce a poor working capacity at small temperature swings (Figure S1). Recently, the utilization of metal−organic frameworks (MOFs) for water sorption was proposed,[41,42] and their diverse structures and tunable properties make them able to meet the specific requirements of various applications, such as atmospheric water harvesting,[43] refrigeration,[44] and heat pump.[45] Apart from the superiority of a large water sorption capacity, MOFs have the desirable "S"-shaped water sorption isotherms allowing reversible sorption−desorption with small temperature or pressure swings. Here we screen out the MIL-101(Cr) ($Cr_3F(H_2O)_2O[(O_2C)-C_6H_4-(CO_2)]_3{\cdot}nH_2O$) from common MOFs as one of the most promising candidates for BTM due to its moderate transition temperature, high thermal stability, fast water sorption/desorption kinetics, and large water sorption capacity in typical climates of 80% relative humidity (RH) at 10 °C (∼1.0 kPa vapor pressure) in winter and 70% RH at 30 °C (∼3.0 kPa vapor pressure) in summer.

We synthesize MIL-101(Cr) by using a hydrothermal method and design a sorption-based SBTM system with the MOF. The powder X-ray diffraction (PXRD) pattern shows that the synthesized MIL-101(Cr) has satisfactory purity (Figure S2), and its pore volume is determined to be as high as 1.74 cm^3/g together with a large BET surface area of 2719.3 m^2/g, according to the results of N_2 gas adsorption (Figure S3). Because the thermal conductivity of MIL-101(Cr) is as low as 0.2 W/m·K (Figure S4), carbon foam (CF) is employed as a thermal conduction enhancement for MIL-101(Cr). The CF is pretreated; then, the well-distributed suspension of MIL-101(Cr) is sprayed onto the CF frameworks to obtain the composite sorbent of MOF@CF (See the detailed information in the Methods section). The results measured by the laser flash method show that MOF@CF exhibits a high thermal conductivity of 0.9 W/(m·K), approximately four to five times higher than that of pristine MIL-101(Cr). Moreover, both water sorption−desorption cycling tests under SBTM work conditions (Figure S5) and falling tests under shaky operation conditions (Figure S6) confirm the MOF@CF has excellent stability. Because of the relatively low desorption temperature (<50 °C) under SBTM work conditions, the water sorption−desorption capacity of MIL-101(Cr) is slightly lower than its saturated sorption capacity, where the coordinated water cannot be released at such low temperatures, as verified by Fourier-transform infrared (FT-IR) spectra of MIL-101(Cr) under different temperatures (Figure S7). Afterward, the MOF@CF is coated on the external surface of a cylindrical LIB as a sorption material for thermal management, and highly thermally conductive tape is used as a thermal interface material (TIM) to reduce the thermal contact resistance between the LIB and MOF@CF (Figure 2a). A thermal resistance and capacity network is given to show the heat transfer conditions from the MOF to ambient air (Figure S8), where the composite sorbent plays a key role in absorbing/generating heat through water desorption/sorption, which is triggered by the ambient temperature or vapor pressure. Because of the contribution of highly thermally conductive carbon foam to accelerate the heat transfer, the conduction resistance of the composite sorbent of MOF@CF (0.001 $m^2{\cdot}K/W$) is one or two orders of magnitude lower than the convective heat transfer coefficient of air (0.01 to 0.1 $m^2{\cdot}K/W$).

An optical image (Figure 2b) shows the good distribution of MIL-101(Cr) on the CF frameworks, while scanning electron microscopy (SEM, Figure 2c,d) and transmission electron microscopy (TEM, Figure 2e) images show that MIL-101(Cr) has satisfactory crystallization and ordered micropores. In the heating mode in winter, MIL-101(Cr) shows a water sorption−desorption transition temperature at 20−30 °C (Figure 2f), indicating that the potential temperature increase of the MOF in the start-up preheating stage is as high as 10 °C due to heat generation from water sorption. Its transition temperature becomes high at 35−45 °C in summer because the water humidity of the air is higher than that in winter. Considering that the optimal working temperature of LIBs is between 20 and 40 °C, MIL-101(Cr) shows the ability to supply both heating and cooling effects under extreme conditions. Additionally, the large water sorption/desorption capacity of ∼1.0 g/g for a small temperature swing indicates its high thermal energy density of 2541 kJ/kg (Figure S9), which is much higher than the energy densities based on conventional solid−liquid or liquid−gas phase-change processes.[47] To show the sorption−desorption transition temperatures under various climate conditions, we provide a series of water sorption isotherms/isobars of MIL-101(Cr) at different pressures and temperatures (Figure S10). To confirm the water sorption capacity of MIL-101(Cr) coated on CF, thermogravimetric analysis (TGA) was carried on both the pure MIL-101(Cr) and the MIL-101(Cr)@CF (Figure S11). The results show the MIL-101(Cr)@CF has a lower desorption temperature, a faster desorption rate, and more thorough release of water compared with bulk pure MIL-101(Cr), indicating that the heat and mass transfer performance was apparently enhanced when it was coated on the frameworks of CF. Remarkably, this sorption-based SBTM system using MIL-101(Cr) can achieve self-regeneration by adsorbing water from air in many major large cities worldwide (Figure 2g), indicating its ability to be widely adopted in worldwide regions. Notably, the selection of MOFs is flexible according to the operation climate, and more hydrophilic MOFs (e.g., MOF-841 or CAU-10) are desirable for reliable self-regeneration in arid regions.[48] Moreover, temperature-sensitive MOFs or hydrogels are also suitable for sorption-based SBTM. Additionally, an auxiliary humidification device for increasing the RH of ambient air can ensure the successful self-regeneration of MOFs under extremely low-humidity conditions.

Proof-of-Concept of Sorption-based Smart Battery Thermal Management. To verify the feasibility of sorption-based SBTM, we first demonstrate a proof-of-concept device for smart thermal management using an electric heater. The

https://dx.doi.org/10.1021/acscentsci.0c00570
ACS Cent. Sci. 2020, 6, 1542−1554

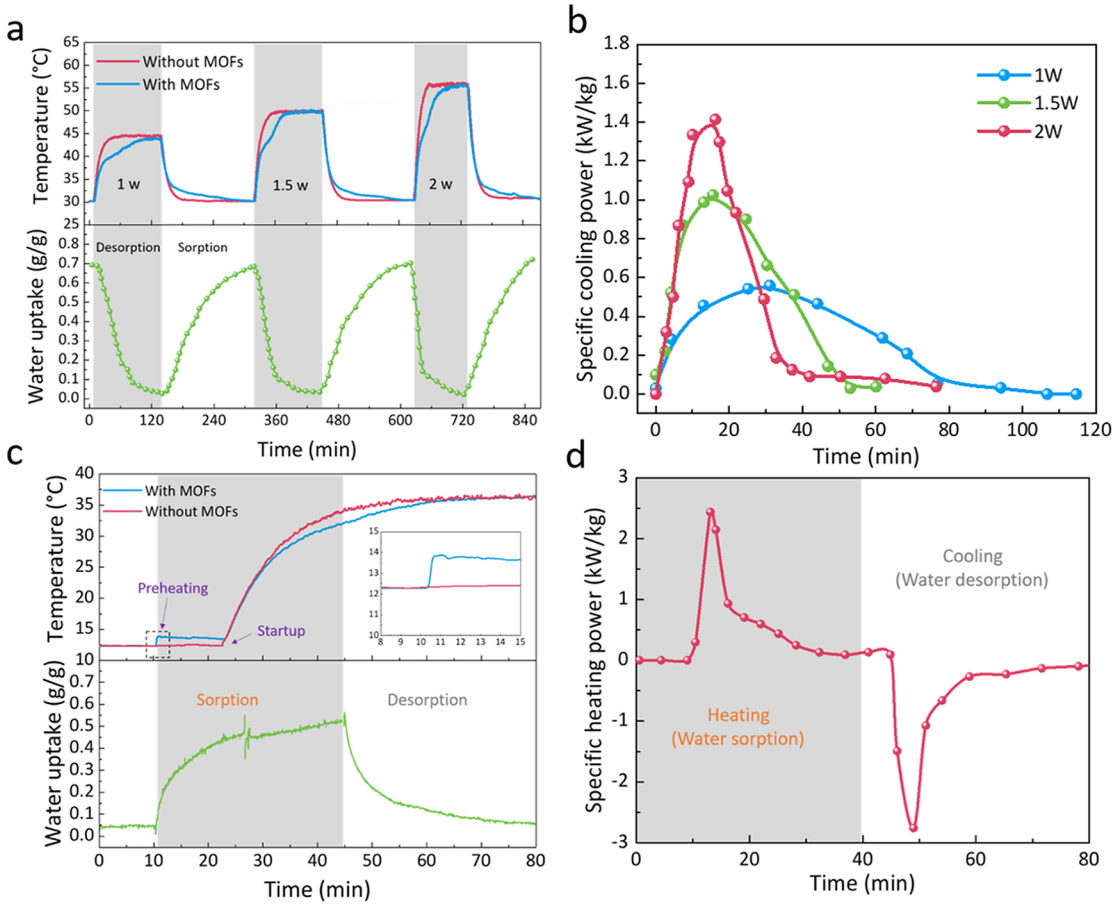

Figure 3. Proof-of-concept of the sorption-based smart thermal management by MOF@CF. (a) Temperature comparison of electric heaters with and without MOF@CF at cooling modes under stable heat generation powers of 1, 1.5, and 2 W, together with the variation of the water uptake of MIL-101(Cr) versus time. Before the tests, the MOF is pretreated to reach its sorption equilibrium completely under ambient conditions; then, the electric heater is powered on. Compared with the blank electric heater without MOF@CF, the other one coated with MOF@CF shows lower temperature during the long operating duration until the amount of water is completely desorbed from the MIL-101(Cr). The MOF can automatically perform self-regeneration when its temperature decreases to the sorption equilibrium temperature after it stops working. (b) Specific cooling power supplied by the water desorption of MIL-101(Cr) at different heating powers, showing the self-adaptive and real-time adjustment of sorption cooling power with different loads. (c) Temperature comparison of two electric heaters during the start-up preheating process at heating mode, together with the variation in water uptake of MIL-101(Cr) versus time. Before the tests, the MIL-101(Cr) is totally dried and isolated from ambient air. The preheating process is triggered by exposing the MOF to air to perform fast water sorption. The hydrated MOF undergoes self-regeneration by the Joule heat generated from electric heater when the operating temperature increases to be higher than the desorption temperature. (d) Specific heating power supplied by the water sorption of MIL-101(Cr) showing the reversible sorption−desorption process for smart thermal management.

electric heater has the same size as 18650 LIBs and can provide a stable heating power from 1 to 2 W to simulate the heat generation power of LIBs under different discharge rates (Figure S12). To reveal the cooling effects of SBTM, we directly compare the temperature profiles of a blank electric heater and an electric heater coated with MOF@CF under a heating process with a constant heating power (Figure 3a). The two electric heaters have almost the same temperature evolution in the beginning stage, and an obvious temperature difference between them appears when the temperature is higher than the desorption temperature of MIL-101(Cr), as shown in Figure 3a. Compared with the blank electric heater, the electric heater coated with MOF@CF has a low temperature due to the heat dissipation by the hydrated MIL-101(Cr) during the water desorption process. The heat consumption of MOF@CF cools the electric heater and dissipates heat to the ambient environment by releasing water vapor to air. A higher heating power brings a sharper temperature increase and a larger temperature difference. Although only 0.51 g of MIL-101(Cr) powder is applied to regulate the working temperature of the electric heater, a maximum temperature difference as high as 8.3 °C is achieved due to its strong cooling effects (Figure S13).

Moreover, the specific cooling power supplied by the water desorption of MIL-101(Cr) exhibits self-adaptive and real-time adjustment at different heating powers (Figure 3b), showing that the cooling power varies with the cooling load from 1 to 2 W. The specific cooling power (q) per mass of the MOF is calculated based on the mass loss of the MOF by the following equation

$$q = \frac{\dot{m}_{\mathrm{MOF}} \cdot \Delta H_{\mathrm{H_2O}}}{m_{\mathrm{MOF}} \cdot M_{\mathrm{H_2O}}} \tag{2}$$

where $\dot{m}_{\mathrm{MOF}}$ is the mass loss rate (water desorption rate) of the MOF, m_{MOF} is the mass of the MOF (0.51 g), $\Delta H_{\mathrm{H_2O}}$ is the

https://dx.doi.org/10.1021/acscentsci.0c00570
ACS Cent. Sci. 2020, 6, 1542−1554

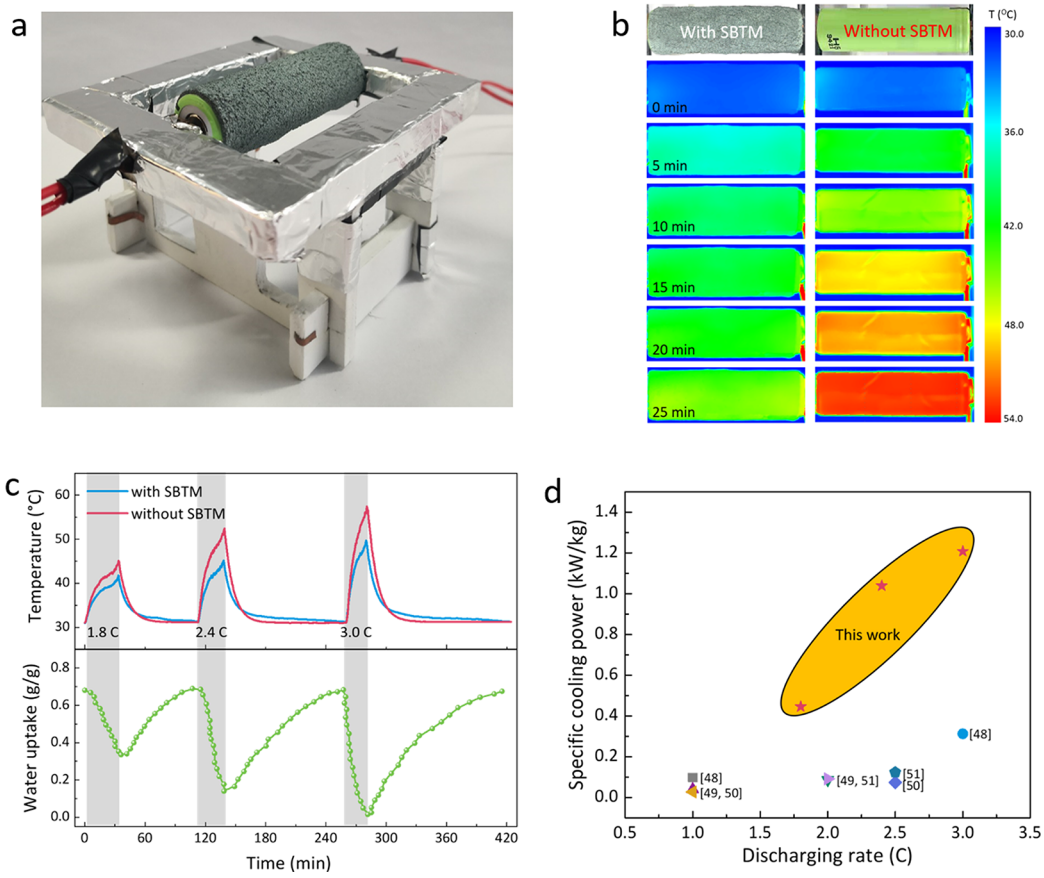

Figure 4. Demonstration of sorption-based smart thermal management to cool commercial 18650 LIBs. (a) Optical image of the 18650 LIB with SBTM. The LIB is covered by the composite sorbent of MOF@CF, whose thickness is 1 mm. (b) Infrared photos showing the temperature evolutions of LIBs with/without SBTM during the discharging phase under a discharging rate of 2.4 C. For the LIB without SBTM, its temperature reaches as high as 54 °C within 25 min and thus has potential safety risks, whereas the LIB with SBTM can be controlled below 45 °C during the whole operating duration. (c) Temperature profiles of LIBs at different discharging rates of 1.8, 2.4, and 3.0 C, showing the strong thermal regulation abilities by the desorption cooling of MIL-101(Cr). Only the partial water inside the MOF is desorbed for cooling at low discharging rates, indicating the water desorption cooling by MIL-101(Cr) is enough to remove all Joule heat generated from a single 18650 LIB at common discharging rates. The faster discharging rate causes a large temperature increase, resulting in faster desorption kinetics together with stronger cooling power, confirming the self-adaptive characteristics of SBTM. (d) Comparison of the cooling powers of the MOF sorption-based SBTM with those of traditional PCM-based BTMs, showing that the SBTM exhibits much higher cooling power and distinct advantages of self-adaptive characteristics with the variation of battery discharging rates. The cooling power can be improved by as high as one order of magnitude.

water desorption enthalpy (44 kJ/mol water), and M_{H_2O} is the relative molecular mass of water.

Because the desorption rate of MIL-101(Cr) is mainly dependent on the driving temperature difference (Figure S14), a higher heating power results in a faster water desorption rate of MIL-101(Cr). Therefore, the high desorption rate increases the amount of water desorbed by the MOF and improves the specific cooling power at a high heating power. After heating, the dry MIL-101(Cr) self-regenerates by adsorbing water from ambient air once its temperature decreases below the sorption equilibrium temperature, as shown in Figure 3a. As a result, hydrated MIL-101(Cr) recovers its water desorption capacity for cooling during the next stage. The dynamic water sorption under different RH conditions shows that the sorption kinetics of MIL-101(Cr) becomes high with increasing RH of air (Figure S15), and thus its self-regeneration duration is positively related to the RH. Moreover, the water uptake of MIL-101(Cr) remains stable (~0.7 g/g) during the sorption−desorption cycles at different heating powers, indicating that sorption-based smart thermal management exhibits reliable heat dissipation for electronic devices by removing the generated heat generation to ambient air in the form of desorption heat of MIL-101(Cr) by releasing water vapor.

For the preheating test, the two electric heaters are placed in cold environments of 12 °C (Figure 3c). Afterward, the temperature of the electric heater coated with MOF@CF rapidly increases to 14 °C once the dry MIL-101(Cr) is exposed to air to enable sorption of atmospheric moisture. The sorption heat released by MIL-101(Cr) preheats the electric heater from a low ambient temperature to a relatively high working temperature. Benefiting from the fast water sorption rate, the temperature increase period is as short as 1 min, which is desirable for fast start-up EVs after short-term preheating. Theoretically, the temperature increase range in the heating mode is close to the temperature decrease range in the cooling mode because the sorption heat of MIL-101(Cr) is close to its desorption heat. However, the heating temperature is much lower than the predicted value in Figure 2f, which is ascribed to the large amount of sorption heat lost to the ambient cold air. The cooling power and heating power in these two modes can be described by the following equations

https://dx.doi.org/10.1021/acscentsci.0c00570
ACS Cent. Sci. 2020, 6, 1542−1554

$$Q_{cooling} = Q_{desorption} + Q_{conv} \quad (3)$$

$$Q_{heating} = Q_{sorption} - Q_{conv} \quad (4)$$

In the cooling mode, as listed in eq 3, the Joule heat generated from the electric heater is not only consumed by the water desorption of MIL-101(Cr) ($Q_{desorption}$) but also dissipated to ambient air by thermal convection (Q_{conv}). Thus the total cooling capacity is the sum of the desorption heat and the convective heat. Because the mass of the composite sorbent is much smaller than that of the battery, the sensible heat caused by temperature changes in the sorbent can be ignored. However, the heating capacity is only supplied by the water sorption heat of MIL-101(Cr) ($Q_{sorption}$) in the heating mode. The sorption heat released by the MOF provides the sensible heat consumed by the device during the preheating stage, but it is also dissipated to the ambient air by thermal convection (Q_{conv}), thus causing a relatively weak heating effect. Therefore, thermal insulation is necessary to further increase the preheating temperature range in cold environments.

As illustrated in Figure 3d, the dry MIL-101(Cr) first undergoes water sorption from air to preheat the electric heater during the low-temperature start-up period, showing a very high transient heating power (~2.5 W/g) in the beginning stage. The sorption heating power provided by the MOF gradually decreases with the temperature increase in the electric heater during its operation phase. At the same time, the Joule heat generated from the electric heater further self-heats it to a high operating temperature. The sorption heating power will be close to zero when the operating temperature reaches the sorption equilibrium temperature of MIL-101(Cr). Afterward, the hydrated MIL-101(Cr) will self-regenerate due to the Joule heat generated from the electric heater. Once the operating temperature of the electric heater increases to above the sorption equilibrium temperature, the hydrated MIL-101(Cr) will undergo water desorption for its regeneration by releasing water vapor to air to become the dry MOF. The self-regeneration through the desorption process makes the dehydrated MIL-101(Cr) recover its water sorption capacity for heating during the next stage, and this can also prevent overheating of the electronic device under extreme operating conditions.

According to the working principle in Figure 1b, the water desorption in the cooling mode is driven by the temperature difference between T_{over} and $T_{B,s}$, whereas the water sorption in the heating mode is driven by the water vapor pressure difference between P_{win} and P_a. The equilibrium characteristics of the MOF powered by temperature or pressure differences ensure that the sorption-based smart thermal management system exhibits the distinct advantages of desorption cooling at high temperatures and sorption heating at low temperatures. In addition, the high sorption heating and cooling powers in Figure 3d indicate that MOF@CF not only enhances the heat transfer between MIL-101(Cr) and electronic devices due to its high thermal conductivity but also improves the mass transfer between MIL-101(Cr) and water vapor due to its porous matrix.

Sorption-based Smart Battery Thermal Management Demonstration. As a preliminary demonstration, we test the sorption-based SBTM performance of the thermal management for a single commercial 18650 LIB under natural air convection conditions (Figure 4a). First, we carry out desorption cooling experiments by comparing the temperature evolutions of a blank LIB and an LIB with SBTM under a common humidity of 60% RH in summer, where the latter shows a lower temperature and a more uniform temperature distribution in IR images under a discharge rate of 2.4 C (Figure 4b). With the strong heat dissipation effects due to the water desorption cooling of MIL-101(Cr), the working temperature of the LIB with SBTM can be effectively controlled below 45 °C during the entire operation duration at the discharge rates of 1.8 and 2.4 C (Figure 4c). Moreover, the working temperature can still remain below 50 °C, even when the discharge rate of the LIB is as high as 3 C, where the maximum temperature difference between the LIB with SBTM and the blank LIB reaches 8.3 °C. In particular, we observe that only part of the water in MIL-101(Cr) (~0.5 g/g) is desorbed for cooling during the LIB discharging process under relatively low discharge rates of 1.8 and 2.4 C according to the mass change of MIL-101(Cr) (Figure 4c), indicating that the SBTM system will never be exhausted before the electricity of the LIB is exhausted. The results indicate that the water desorption cooling by 0.51 g MIL-101(Cr) is sufficiently high to cover all Joule heat generated from a single 18650 LIB at common discharge rates. The contributions from the sensible heats of the MOF and CF are <5% due to the high desorption enthalpy of the MOF (Table S1). Moreover, the comparison tests between the blank battery and the pure CF confirm that the cooling effects from CF are small enough to be ignored (Figure S16). More importantly, the weight of the MOF is only 1.0% of the weight of the battery (48 g for the LIB), but >60 g paraffin wax is needed for traditional PCM-based BTM, indicating the distinct advantage of high-energy/power-density BTM in our strategy. To improve the reliability of SBTM under some extreme conditions, such as continuous charging−discharging at high rates, the amount of MIL-101(Cr) can be flexibly adjusted to cover all of the Joule heat (Figures S17 and S18).

Similar to the proof-of concept tests, MIL-101(Cr) can self-regenerate by adsorbing water from air when the LIB stops working. Approximately 1 to 2 h is required to complete the self-regeneration process during the natural cooling of the LIB in this test; however, the self-regeneration duration can be significantly shortened if forced air convection is introduced by improving the sorption heat dissipation and water molecule diffusion to ambient air. Moreover, the influence of the RH on the desorption cooling performance shows that the MOF sorption-based SBTM is still strong for the efficient thermal management of the commercial 18650 LIB under high humidity, even at 80% RH (Figure S19). In comparison with traditional PCM-based BTM methods, our MOF sorption-based SBTM system shows a much higher cooling power at different discharge rates due to the ultrahigh solid−gas sorption reaction enthalpy of MIL-101(Cr), and the cooling power can be improved by as high as one order of magnitude (Figure 4d).[48−51] Moreover, the sorption-based SBTM exhibits the desirable self-adaptive characteristics of the cooling power with the variation in the battery cooling load at different discharge rates, whereas traditional PCM-based BTM methods nearly maintain a stable cooling power because of the fixed phase-change temperature, resulting in a nearly constant heat transfer power. Remarkably, the proposed SBTM can automatically adjust the cooling power between 0 and 1.2 kW/kg according to the real-time temperature of the battery under practical operating conditions, such as the typical driving conditions of an EV given by the Federal Urban Driving

https://dx.doi.org/10.1021/acscentsci.0c00570
ACS Cent. Sci. 2020, 6, 1542−1554

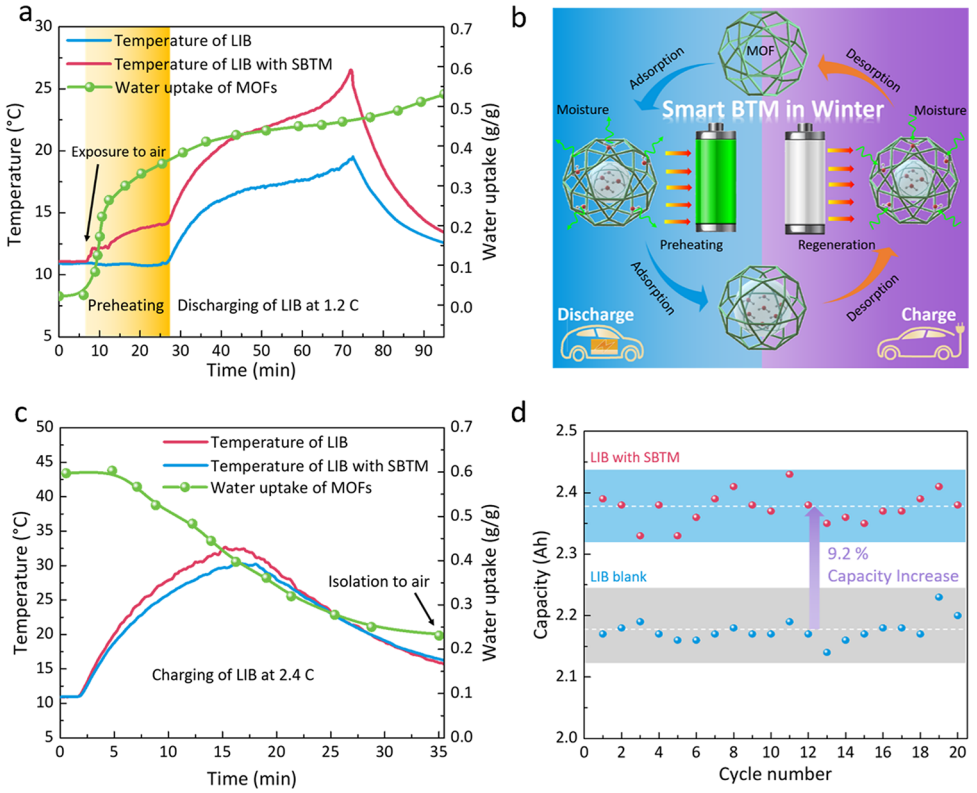

Figure 5. Concept design and feasibility testing of sorption-based smart thermal management to heat commercial 18650 LIBs. (a) Temperature profiles of LIBs with and without MOF@CF during the preheating and discharging process, together with the variation in water uptake of MIL-101(Cr) versus time. A temperature increase of 3 °C is realized before the start-up of the LIB, together with a further temperature increase of 5 °C during the battery discharging phase. (b) Schematic of the reversible heating process of LIBs with a periodical water desorption regeneration strategy. Before LIBs start-up, the dry MOF is exposed to air to adsorb water from moisture, releasing sorption heat to heat the LIBs. After several minutes, the LIBs begin to discharge, and the MOF continuously adsorbs water until it reaches a saturated state, bringing a further temperature increase in LIBs. (c) Temperature comparison of LIBs with and without MOF@CF during the 2.4 C charging process, together with the variation in water uptake of MIL-101(Cr) versus time. The temperature of the LIB with SBTM becomes low during the high-rate charging to avoid the overheating of the LIB, and the Joule heat generation is used for the regeneration of MOF@CF. (d) Comparison of the battery capacities of the LIB with and without SBTM, showing that the apparent battery capacity of the LIB with SBTM can be increased by 9.2% and indicating that warm working temperature allows the LIB to more deeply discharge−charge.

Schedule (FUDS), where the highest discharge rate during the rapid acceleration process is ∼2 C (∼45 A) and the average discharge rate during the entire driving process is only 0.2 C (∼4.5 A) (Figure S20). We further designed and constructed an LIB pack with 4S (four cells in series) to confirm the feasibility of SBTM in the LIB pack, where four LIBs are staggered and arranged as 2*2 with 10 mm gaps between each other, as shown in Figure S21. During the discharge process under 3 C, the temperature of the LIB pack with SBTM is 10 °C lower than that of the LIB pack without SBTM following a 0.45 g/g water desorption, confirming that the SBTM can efficiently operate under the LIB pack with narrowed space. Additionally, forced air convection can also be used to further improve the mass transfer and promote the water vapor diffusion from the LIB to an ambient environment if needed. To confirm the stability of MIL-101(Cr)@CF, the PXRD pattern of the MIL-101(Cr) after 10 operating cycles was compared with that of the original synthesized MIL-101(Cr), whose results show that the crystal structure remains stable (Figure S22). Moreover, the SEM images also confirm that the morphology of MIL-101(Cr) remains the same as the original MIL-101(Cr) (Figure S23). Consequently, the MOF sorption-based SBTM provides a potential strategy to realize efficient battery cooling with the distinct advantages of smart self-adaptive adjustment, near-zero energy consumption, low-cost operation, and high energy density.

In cold environments, the electrolyte viscosity increases and thus impedes the movement of charge carriers. Under extremely cold conditions, the electrolyte even freezes and causes the battery to be unable to discharge and the EV to be unable to start. Additionally, the energy and power of LIBs are substantially reduced at low temperatures. Therefore, preheating LIBs before start-up and maintaining moderate temperatures during the operation phase are key points for BTM in winter. Here we demonstrate heating applications of SBTM for the thermal management of a commercial 18650 LIB in a cold environment of 10 °C. The IR images show that the sorption heat released by MIL-101(Cr) during its water sorption from air can effectively raise the temperature of the LIB and ensure a uniform temperature distribution in the start-up stage (Figure S24). However, much heat is lost to the surrounding environment at the edge parts of the LIB, which causes the temperature increase of the LIB during the heating process to be small (<3 °C). To enlarge the temperature increase, we design a semiclosed SBTM system to reduce the heat loss by preventing heat dissipation to cold air as much as possible while allowing water vapor transport between MIL-101(Cr) and the air atmosphere (Figure S25). The total temperature

https://dx.doi.org/10.1021/acscentsci.0c00570
ACS Cent. Sci. 2020, 6, 1542−1554

increase achieved by the water sorption heat of MIL-101(Cr) is as high as 8 °C in the semiclosed SBTM system (Figure 5a), including a temperature increase of 3 °C in the preheating stage and a further temperature increase of 5 °C in the discharging phase. Therefore, the semiclosed sorption-based SBTM system exhibits efficient sorption heating for the thermal management of LIBs at low temperatures. Moreover, benefiting from the fast sorption kinetics of the MOF and its large sorption heat released in the initial stage, the preheating time is as short as several minutes, which is desirable for fast start-up in winter. However, Joule heat generated by the LIB during the operation process is not sufficient for driving the regeneration of MIL-101(Cr) at a low discharge rate, and thus achieving self-regeneration by the internal Joule heat from LIBs is difficult.

To address this challenge, we propose a method for the regeneration of MIL-101(Cr) by utilizing the heat utilization generated from LIBs during both the discharging and charging processes, as illustrated in Figure 5b. During the discharging process in cold environments (left part), the water sorption heat released by MIL-101(Cr) heats the LIB from a low temperature to a suitable working temperature in the start-up and early operation stages of the discharging process. Afterward, MIL-101(Cr) begins its self-regeneration, desorbing water vapor to air by utilizing the Joule heat generation of the LIB until it completes the whole discharging process. During the charging process (right part), the MOF desorbs the residual water to air by recovering the heat generated by the LIB because the charging process is generally continuous. To ensure the complete regeneration of the MOF, alternating current (AC) electrothermal conversion from the battery charging station can be used to actively drive the water desorption of MIL-101(Cr). The water content of MIL-101(Cr) can be easily detected based on the remarkably variation in the impedance before and after desorbing water,[52] which guides whether extra electrothermal input is needed after battery charging. Even if the MOF is completely regenerated by consuming external electricity, the sorption-induced heating strategy still has the advantages of a fast temperature response rate and a larger thermal energy storage density (706 Wh/kg for MIL-101(Cr)) compared with the electricity storage density of LIBs (<350 Wh/kg) in this stage.[53]

We further evaluate the feasibility of the combined discharging−charging heat generation method and find that hydrated MIL-101(Cr) can complete its regeneration within 35 min by using only the internal heat generated by the LIB during the battery charging process at 2.4 C (Figure 5c). After regeneration, the semiclosed SBTM system is closed to isolate the humidity in the air from the MOF, which will be reopened to the air in the next stage to perform water sorption to preheat the LIB. The overnight isolation of the MOF from air requires good sealing of the battery, and thus an air inlet valve controlling the access of moisture is necessary for practical applications. The regeneration of MIL-101(Cr) can also prevent the overheating problem of LIBs during the charging stage at high rates by consuming heat in the form of the desorption heat of MIL-101(Cr). Benefiting from the preheating and suitable working temperature of the LIB in cold environments, the working capacity of the battery with SBTM can be improved by 9.2% compared with that of the battery without SBTM, as shown in Figure 5d, which means that the sorption-based SBTM can enlarge the driving range by ∼37 km on the assumption of a 400 km travel distance for common EVs in winter. Notably, the mass and heat transfer conditions of the battery pack are different for different EVs, and thus more efforts need to be focused on engineering innovations to take the proposed SBTM strategy from concept design to practical application in the future.

CONCLUSIONS

In summary, we reported a near-zero-energy SBTM strategy to regulate the battery temperature in both hot and cold environments enabled by sorption energy harvesting from air. The sorption-based SBTM can overcome the contradiction of cooling requirements at high temperatures and heating requirements at low temperatures for BTM. The sorption-induced endothermic/exothermic effects enable passive battery cooling/heating through reversible water vapor desorption/sorption of the sorbent without any additional energy input. The liquid-free operation makes the sorption-based SBTM very suitable for the thermal management of electronic devices/batteries. We further demonstrated SBTM applications for the thermal management of commercial 18650 LIBs with MIL-101(Cr)@CF. The sorption-based SBTM system can control the battery temperature below 45 °C, even at a high discharge rate of 3 C in a hot environment while realizing self-preheating to ∼15 °C in a cold environment, with an increase in battery capacity of 9.2%. Importantly, the SBTM strategy can automatically switch between the battery cooling and heating modes by realizing the self-regeneration of MIL-101(Cr) between its hydrated and dehydrated states via water vapor sorption from air or desorption to air. Moreover, the sorption-based SBTM exhibits self-adaptive working powers with variation in the battery temperature and an ultrahigh power density compared with the traditional PCM-based BTM methods, improved by one order of magnitude. Our proposed sorption-based SBTM strategy has the distinct advantages of being a liquid-free, high-energy/power-density, near-zero energy consumption, low-operating-cost, and self-adaptive smart thermal management approach for electronic devices/batteries.

METHODS

Synthesis and Characterization of MIL-101(Cr) and MOF@CF. First, 0.01 mol chromic nitrate nona-hydrate and 0.01 mol terephthalic acid were added to 47.5 mL of deionized water; then, the mixture was stirred for 15 min at room temperature. Afterward, the mixed solution was transferred to a 100 mL Teflon vessel and heated to 220 °C for 8 h for the self-assembly synthesis of MIL-101(Cr) crystals.[54] The residual terephthalic acid inside the MIL-101(Cr) pores was washed with DMF, ethanol, and deionized water three times to obtain a pure MIL-101(Cr) suspension. The MOF@CF composite was prepared by spraying the MIL-101(Cr) suspension into CF pores using an electric spray gun. During the spraying process, the composite was heated to 80 °C for 30 min per 10 mL of MIL-101(Cr) suspension sprayed; finally 0.51 g of MIL-101(Cr) was coated on 2.26 g of CF. The thermal diffusivity of the composite was measured by the laser flash method using a commercial instrument (LFA 447, Netzsch). Carbon was sprayed on the surface to avoid reflection and reduce the roughness before testing. The thermal capacity (C_p) of the dry composite sorbent was measured by using differential scanning calorimetry (Pyris1 DSC, PerkinElmer). The morphology of

https://dx.doi.org/10.1021/acscentsci.0c00570
ACS Cent. Sci. 2020, 6, 1542−1554

MIL-101(Cr)@CF was characterized by a field-emission scanning electron microscope (FESEM, Sirion 200 instrument, FEI). The PXRD patterns were measured by an X-ray diffractometer (Ultima IV, Rigaku). N_2 gas adsorption was measured with a gas sorption analyzer (Autosorb-IQ3, Quantachrome) at 77 K. FT-IR spectra were measured by an FT-IR spectrometer (Nicolet 6700, Thermo Fisher Scientific) with varying temperatures from 25 to 45 °C. The TGA tests were carried out by a commercial thermogravimetric analyzer (STA 449, Netzsch) equipped with a moisture humidity generator (MHG 32, ProUmid). The samples of pure MOF and MOF@CF first reached the water sorption equilibrium at 30 °C, 60% RH (water vapor pressure of 2.55 kPa). Then, the samples were heated from 30 to 120 °C at a constant heating rate of 0.2 °C/min, under a water vapor atmosphere with a constant vapor pressure of 2.55 kPa, wherein the flow rate of water vapor was 150 mL/min.

Water Sorption Isotherm and Isobar Measurements. The water sorption isotherms were measured using an accelerated surface area and porosimetry analyzer (ASAP 2020, Micromeritics) under a water vapor atmosphere with controllable vapor pressure. The sample temperature was set as a constant (35, 40, and 45 °C), and the relative pressure of the water vapor was increased from 0 to 1 according to a set of pressure intervals. The water sorption isobars were measured using a self-constructed adsorption testing device. First, the MOF samples reached adsorption equilibrium under a specific water vapor pressure (500, 1000, 2000, 3000, 4000, and 5000 Pa, respectively); then, the water vapor pressure inside the gas chamber was kept constant, and the sample temperature was increased according to a set of temperature intervals. Every equilibrium point was determined when the weight change was <0.02% over 10 min. The water sorption−desorption cycling tests were carried out by a commercial thermogravimetric analyzer (STA 449, Netzsch) equipped with a moisture humidity generator (MHG 32, ProUmid) under working conditions of 30 °C at 2.55 kPa (60% RH) for sorption and 45 °C at 2.55 kPa for desorption.

SBTM Demonstration Experiments. For the stable working conditions of the battery, all demonstration experiments were carried out in a psychrometer testing room with a constant temperature and a constant RH. (See the fluctuations of the temperature and RH in Figure S26.) Commercial single-battery online testing equipment with a constant current−constant voltage (CC−CV) protocol (SBCT-3125, QunLing energy) was used for battery charge−discharge. Cooling mode: The batteries with/without SBTM were first fully charged and naturally cooled to room temperature; then, they were discharged at 1.8, 2.4, and 3.0 C at 30 °C and 60% RH. Heating mode: The batteries with/without SBTM were fully charged at 2.4 C, during which the composite sorbents wrapped around the batteries were desorbed. Then, the two batteries were enclosed in a confined space to avoid water adsorption (Figure S25). The confined space was opened, allowing water adsorption before the battery start-up to preheat the batteries to 10 °C and 80% RH. Battery capacity cycling tests were carried out by repeated charging−discharging of two new 18650 LIBs at 10 °C and 80% RH, where one was covered with the MOF and the other was blank. The temperatures of the batteries were measured by highly accurate Pt-100 temperature sensors, which were placed between the MOF and the battery (under the MOF) to directly measure the temperatures of the external surface of the batteries, which were approximately regarded as the temperatures of the batteries. IR thermometry was also used to qualitatively evaluate the uniformity of the temperature distribution at the MOF surface. The mass change of the MOF was measured by an electronic balance (ME503TE, Mettler Toledo), whose real-time values were automatically recorded.

■ ASSOCIATED CONTENT

Supporting Information

The Supporting Information is available free of charge at https://pubs.acs.org/doi/10.1021/acscentsci.0c00570.

Water sorption isobars, thermal conductivities of sorbents, details of experiments, and results of experiments (PDF)

■ AUTHOR INFORMATION

Corresponding Authors

Tingxian Li − *Research Center of Solar Power & Refrigeration, School of Mechanical Engineering, Shanghai Jiao Tong University, Shanghai 200240, China;* orcid.org/0000-0003-4618-8144; Email: Litx@sjtu.edu.cn

Ruzhu Wang − *Research Center of Solar Power & Refrigeration, School of Mechanical Engineering, Shanghai Jiao Tong University, Shanghai 200240, China;* orcid.org/0000-0003-3586-5728; Email: rzwang@sjtu.edu.cn

Authors

Jiaxing Xu − *Research Center of Solar Power & Refrigeration, School of Mechanical Engineering, Shanghai Jiao Tong University, Shanghai 200240, China;* orcid.org/0000-0002-8913-9783

Jingwei Chao − *Research Center of Solar Power & Refrigeration, School of Mechanical Engineering, Shanghai Jiao Tong University, Shanghai 200240, China*

Taisen Yan − *Research Center of Solar Power & Refrigeration, School of Mechanical Engineering, Shanghai Jiao Tong University, Shanghai 200240, China*

Si Wu − *Research Center of Solar Power & Refrigeration, School of Mechanical Engineering, Shanghai Jiao Tong University, Shanghai 200240, China*

Minqiang Wu − *Research Center of Solar Power & Refrigeration, School of Mechanical Engineering, Shanghai Jiao Tong University, Shanghai 200240, China*

Bingchen Zhao − *Research Center of Solar Power & Refrigeration, School of Mechanical Engineering, Shanghai Jiao Tong University, Shanghai 200240, China*

Complete contact information is available at: https://pubs.acs.org/10.1021/acscentsci.0c00570

Author Contributions

†J.X., J.C., and T.L. contributed equally to this work.

Notes

The authors declare no competing financial interest.

■ ACKNOWLEDGMENTS

This work was supported by the National Natural Science Foundation of China under contract no. 51876117 and the National Key R&D Program of China under contract no. 2018YFE0100300. Part of this work was funded by the Innovative Research Group Project of National Natural Science Foundation of China under contract no. 51521004.

We thank Weili Luo for assistance during the thermogravimetric analysis.

REFERENCES

(1) Dunn, B.; Kamath, H.; Tarascon, J. M. Electrical energy storage for the grid: A battery of choices. *Science* **2011**, *334*, 928−935.
(2) Goodenough, J. B.; Park, K. S. The Li-ion rechargeable battery: A perspective. *J. Am. Chem. Soc.* **2013**, *135*, 1167−1176.
(3) Chu, S.; Cui, Y.; Liu, N. The path towards sustainable energy. *Nat. Mater.* **2017**, *16*, 16−22.
(4) Palacín, M. R.; De Guibert, A. Why do batteries fail? *Science* **2016**, *351*, 1253292.
(5) Yang, F.; Xie, Y.; Deng, Y.; Yuan, C. Predictive modeling of battery degradation and greenhouse gas emissions from US state-level electric vehicle operation. *Nat. Commun.* **2018**, *9*, 1−10.
(6) Liu, Y.; Zhu, Y.; Cui, Y. Challenges and opportunities towards fast-charging battery materials. *Nature Energy* **2019**, *4*, 540−550.
(7) Yang, X. G.; Liu, T.; Gao, Y.; Ge, S.; Leng, Y.; Wang, D.; Wang, C. Y. Asymmetric Temperature Modulation for Extreme Fast Charging of Lithium-Ion Batteries. *Joule* **2019**, *3*, 3002−3019.
(8) Waldmann, T.; Wilka, M.; Kasper, M.; Fleischhammer, M.; Wohlfahrt-Mehrens, M. Temperature dependent ageing mechanisms in Lithium-ion batteries - A Post-Mortem study. *J. Power Sources* **2014**, *262*, 129−135.
(9) Deng, J.; Bae, C.; Marcicki, J.; Masias, A.; Miller, T. Safety modelling and testing of lithium-ion batteries in electrified vehicles. *Nature Energy* **2018**, *3*, 261−266.
(10) Zhu, Y.; Xie, J.; Pei, A.; Liu, B.; Wu, Y.; Lin, D.; Li, J.; Wang, H.; Chen, H.; Xu, J.; Yang, A.; Wu, C.-L.; Wang, H.; Chen, W.; Cui, Y. Fast lithium growth and short circuit induced by localized-temperature hotspots in lithium batteries. *Nat. Commun.* **2019**, *10*, 1−7.
(11) Zinth, V.; et al. Lithium plating in lithium-ion batteries at sub-ambient temperatures investigated by in situ neutron diffraction. *J. Power Sources* **2014**, *271*, 152−159.
(12) Rao, Z.; Wang, S. A review of power battery thermal energy management. *Renewable Sustainable Energy Rev.* **2011**, *15*, 4554−4571.
(13) Liu, H.; Wei, Z.; He, W.; Zhao, J. Thermal issues about Li-ion batteries and recent progress in battery thermal management systems: A review. *Energy Convers. Manage.* **2017**, *150*, 304−330.
(14) Chen, J.; et al. Effects of different phase change material thermal management strategies on the cooling performance of the power lithium ion batteries: A review. *J. Power Sources* **2019**, *442*, 227228.
(15) Chen, L.; et al. Electro- and photodriven phase change composites based on wax-infiltrated carbon nanotube sponges. *ACS Nano* **2012**, *6*, 10884−10892.
(16) Cottrill, A. L.; Liu, A. T.; Kunai, Y.; Koman, V. B.; Kaplan, A.; Mahajan, S. G.; Liu, P.; Toland, A. R.; Strano, M. S. Ultra-high thermal effusivity materials for resonant ambient thermal energy harvesting. *Nat. Commun.* **2018**, *9*, 1−11.
(17) Wu, S.; Li, T.; Tong, Z.; Chao, J.; Zhai, T.; Xu, J.; Yan, T.; Wu, M.; Xu, Z.; Bao, H.; Deng, T.; Wang, R. High-Performance Thermally Conductive Phase Change Composites by Large-Size Oriented Graphite Sheets for Scalable Thermal Energy Harvesting. *Adv. Mater.* **2019**, *31*, 1905099.
(18) Al-Zareer, M.; Dincer, I.; Rosen, M. A. Comparative assessment of new liquid-to-vapor type battery cooling systems. *Energy* **2019**, *188*, 116010.
(19) Rao, Z.; Wang, S.; Wu, M.; Lin, Z.; Li, F. Experimental investigation on thermal management of electric vehicle battery with heat pipe. *Energy Convers. Manage.* **2013**, *65*, 92−97.
(20) Al-Zareer, M.; Dincer, I.; Rosen, M. A. Novel thermal management system using boiling cooling for high-powered lithium-ion battery packs for hybrid electric vehicles. *J. Power Sources* **2017**, *363*, 291−303.
(21) Ren, Y.; Yu, Z.; Song, G. Thermal management of a Li-ion battery pack employing water evaporation. *J. Power Sources* **2017**, *360*, 166−171.
(22) Fang, G.; et al. Thermal management for a tube-shell Li-ion battery pack using water evaporation coupled with forced air cooling. *RSC Adv.* **2019**, *9*, 9951−9961.
(23) Wang, C.; Hua, L.; Yan, H.; Li, B.; Tu, Y.; Wang, R. A Thermal Management Strategy for Electronic Devices Based on Moisture Sorption-Desorption Processes A Thermal Management Strategy for Electronic Devices Based on Moisture Sorption-Desorption Processes. *Joule* **2020**, *4*, 435.
(24) Mishra, A. K.; et al. Autonomic perspiration in 3D-printed hydrogel actuators. *Science Robotics* **2020**, *5*, eaaz3918.
(25) Li, R.; Shi, Y.; Wu, M.; Hong, S.; Wang, P. Photovoltaic panel cooling by atmospheric water sorption−evaporation cycle. *Nat. Sustain.* **2020**, *3*, 636−643.
(26) Hu, X.; et al. Battery warm-up methodologies at subzero temperatures for automotive applications: Recent advances and perspectives. *Prog. Energy Combust. Sci.* **2020**, *77*, 100806.
(27) Wang, T.; et al. Performance of plug-in hybrid electric vehicle under low temperature condition and economy analysis of battery pre-heating. *J. Power Sources* **2018**, *401*, 245−254.
(28) Hao, M.; Li, J.; Park, S.; Moura, S.; Dames, C. Efficient thermal management of Li-ion batteries with a passive interfacial thermal regulator based on a shape memory alloy. *Nature Energy* **2018**, *3*, 899−906.
(29) Wang, C. Y.; et al. Lithium-ion battery structure that self-heats at low temperatures. *Nature* **2016**, *529*, 515−518.
(30) Li, T. X.; Wang, R. Z.; Li, H. Progress in the development of solid-gas sorption refrigeration thermodynamic cycle driven by low-grade thermal energy. *Prog. Energy Combust. Sci.* **2014**, *40*, 1−58.
(31) Yu, N.; Wang, R. Z.; Wang, L. W. Sorption thermal storage for solar energy. *Prog. Energy Combust. Sci.* **2013**, *39*, 489−514.
(32) Dawoud, B.; Aristov, Y. Experimental study on the kinetics of water vapor sorption on selective water sorbents, silica gel and alumina under typical operating conditions of sorption heat pumps. *Int. J. Heat Mass Transfer* **2003**, *46*, 273−281.
(33) Gur, I.; Sawyer, K.; Prasher, R. Searching for a better thermal battery. *Science* **2012**, *335*, 1454−1455.
(34) Kim, H.; Yang, S.; Rao, S. R.; Narayanan, S.; Kapustin, E. A.; Furukawa, H.; Umans, A. S.; Yaghi, O. M.; Wang, E. N. Water harvesting from air with metal-organic frameworks powered by natural sunlight. *Science* **2017**, *356*, 430−434.
(35) Tu, Y.; Wang, R.; Zhang, Y.; Wang, J. Progress and expectation of atmospheric water harvesting. *Joule* **2018**, *2*, 1452−1475.
(36) Rieth, A. J.; Yang, S.; Wang, E. N.; Dincă, M. Record atmospheric fresh water capture and heat transfer with a material operating at the water uptake reversibility limit. *ACS Cent. Sci.* **2017**, *3*, 668−672.
(37) Nandakumar, D. K.; et al. A super hygroscopic hydrogel for harnessing ambient humidity for energy conservation and harvesting. *Energy Environ. Sci.* **2018**, *11*, 2179−2187.
(38) Yang, L.; Nandakumar, D. K.; Miao, L.; Suresh, L.; Zhang, D.; Xiong, T.; Vaghasiya, J. V.; Kwon, K. C.; Ching Tan, S. Energy harvesting from atmospheric humidity by a hydrogel-integrated ferroelectric-semiconductor system. *Joule* **2020**, *4*, 176−188.
(39) Thommes, M.; et al. Physisorption of gases, with special reference to the evaluation of surface area and pore size distribution (IUPAC Technical Report). *Pure Appl. Chem.* **2015**, *87*, 1051−1069.
(40) Xu, J. X.; Li, T. X.; Chao, J. W.; Yan, T. S.; Wang, R. Z. High energy-density multi-form thermochemical energy storage based on multi-step sorption processes. *Energy* **2019**, *185*, 1131−1142.
(41) Wang, S.; et al. A robust large-pore zirconium carboxylate metal−organic framework for energy-efficient water-sorption-driven refrigeration. *Nature Energy* **2018**, *3*, 985−993.
(42) Rieth, A. J.; et al. Record-Setting Sorbents for Reversible Water Uptake by Systematic Anion Exchanges in Metal-Organic Frameworks. *J. Am. Chem. Soc.* **2019**, *141*, 13858−13866.

https://dx.doi.org/10.1021/acscentsci.0c00570
ACS Cent. Sci. 2020, 6, 1542−1554

(43) Hanikel, N.; et al. Rapid Cycling and Exceptional Yield in a Metal-Organic Framework Water Harvester. *ACS Cent. Sci.* **2019**, *5*, 1699−1706.
(44) Lenzen, D.; Bendix, P.; Reinsch, H.; Frohlich, D.; Kummer, H.; Mollers, M.; Hugenell, P. P. C.; Glaser, R.; Henninger, S.; Stock, N. Scalable Green Synthesis and Full-Scale Test of the Metal−Organic Framework CAU-10-H for Use in Adsorption-Driven Chillers. *Adv. Mater.* **2018**, *30*, 1705869.
(45) Rieth, A. J.; et al. Tunable metal-organic frameworks enable high efficiency cascaded adsorption heat pumps. *J. Am. Chem. Soc.* **2018**, *140*, 17591−17596.
(46) Historical weather: Weather Underground. https://www.wunderground.com.
(47) De Lange, M. F.; Verouden, K. J. F. M.; Vlugt, T. J. H.; Gascon, J.; Kapteijn, F. Adsorption-Driven Heat Pumps: The Potential of Metal-Organic Frameworks. *Chem. Rev.* **2015**, *115*, 12205−12250.
(48) Li, W. Q.; Qu, Z. G.; He, Y. L.; Tao, Y. B. Experimental study of a passive thermal management system for high-powered lithium ion batteries using porous metal foam saturated with phase change materials. *J. Power Sources* **2014**, *255*, 9−15.
(49) Lin, C.; Xu, S.; Chang, G.; Liu, J. Experiment and simulation of a $LiFePO_4$ battery pack with a passive thermal management system using composite phase change material and graphite sheets. *J. Power Sources* **2015**, *275*, 742−749.
(50) Lv, Y.; et al. Experimental study on a novel battery thermal management technology based on low density polyethylene-enhanced composite phase change materials coupled with low fins. *Appl. Energy* **2016**, *178*, 376−382.
(51) Azizi, Y.; Sadrameli, S. M. Thermal management of a $LiFePO_4$ battery pack at high temperature environment using a composite of phase change materials and aluminum wire mesh plates. *Energy Convers. Manage.* **2016**, *128*, 294−302.
(52) Zhang, J.; Sun, L.; Chen, C.; Liu, M.; Dong, W.; Guo, W.; Ruan, S. High performance humidity sensor based on metal organic framework MIL-101 (Cr) nanoparticles. *J. Alloys Compd.* **2017**, *695*, 520−525.
(53) Lee, J. H.; et al. High-energy-density lithium-ion battery using a carbon-nanotube−Si composite anode and a compositionally graded $Li[Ni_{0.85}Co_{0.05}Mn_{0.10}]O_2$ cathode. *Energy Environ. Sci.* **2016**, *9*, 2152−2158.
(54) Seo, Y. K.; et al. Energy-efficient dehumidification over hierachically porous metal-organic frameworks as advanced water adsorbents. *Adv. Mater.* **2012**, *24*, 806−810.

https://dx.doi.org/10.1021/acscentsci.0c00570
ACS Cent. Sci. 2020, 6, 1542−1554